SOL ENGINEERING SERVICES

Carbon Fiber Composite Target Plates for High-Heat-Flux Cooling

Fiber and composite thermal conductivity, through-thickness fiber orientation, printed pitch-fiber limits, thermoplastic matrices in hot coolant, plating adhesion, jet erosion and tests of the CF-JET target-plate claims

Prepared for DEVCOM Army Research Laboratory, the Ground Vehicle Systems Center, and university and industry partners of the CF-JET effort

Classification	Unclassified. Prepared from open-source information.
Date	23 November 2026

Executive Summary

A carbon fiber target plate can conduct heat through its thickness at 50 W/m·K or more only if continuous high-conductivity fiber stands perpendicular to the plate at a volume fraction of roughly 6 to 9 percent, and no published measurement of a millimeter-thick insert at that level was found. The reported measurements that come closest are thin elastomer interface materials with vertically aligned pitch fiber, which reach 35.2 to 51.9 W/m·K.[12] Standard laminates of carbon fiber in epoxy conduct 0.76 to 2.8 W/m·K through the thickness at 51.6 to 74.5 percent fiber, including laminates made with K13D2U pitch fiber.[34] The CF-JET design point of 1.5 kW on 36 cm² and 0.02 K/W equals 72 mm²·K/W, and the claims about the target plate decide how much of that budget the plate consumes.[5]

- **Fiber conductivity.** Pitch fiber conducts 140 to 1,000 W/m·K along its axis by vendor value, and the measured values are lower: 576 W/m·K for K1100 at 27 °C and 768 to 792 W/m·K for K13D2U tows.[67] PAN fiber conducts 8.8 to 65.2 W/m·K, and across the fiber the conductivity is 3 to 21 percent of the axial value for the PAN fibers measured (derived from reported ratios, Table 1, Figure 2).[8]
- **Through-thickness requirement.** A parallel-conduction estimate gives a perpendicular fiber volume fraction of 6.2 percent for 50 W/m·K and 37.5 percent for 300 W/m·K with an ideal 800 W/m·K fiber. At 70 percent efficiency the fractions are 8.9 and 53.5 percent (derived, Table 3).
- **Printing limits.** The best printed continuous pitch fiber sample reached 36.63 W/m·K at 6.42 percent fiber, about 30 percent under the parallel estimate, and that fiber fraction is the practical ceiling reported for the process.[9] No documentation of commercial printers processing pitch fiber was found, and typical printed laminates hold 12 percent voids.[10]
- **Matrices.** PEEK showed no mass change in 90 days of hot water at 120 to 160 °C, while nylon 66 lost up to 65 percent of its molar mass in 336 hours in water-glycol at 140 °C (Table 6).[1112] No PEKK data in hot water-glycol were found.
- **Plated face.** Copper at 10 to 25 µm adds 0.025 to 0.0625 mm²·K/W, or 0.03 to 0.09 percent of the budget (derived). A 50 µm polymer skin adds 0.0556 K/W at 0.25 W/m·K, which is 2.8 times the entire 0.02 K/W budget (derived, Figure 5).
- **Erosion.** No erosion rate for a polymer under a liquid jet slower than 10 m/s was found. The published water-jet test used about 173 m/s, which is 25.5 times the 6.8 m/s of a 0.5 mm jet at 8 L/min (derived, Table 8).[13]

The implications for CF-JET are specific. At 36 W/m·K, a 1 mm insert uses 28 mm²·K/W and a 2 mm insert uses 55 mm²·K/W of the 72 mm²·K/W budget (derived). A 50 µm skin on the jet side adds 172 mm²·K/W at the conductivity of unfilled PEEK and exceeds the budget by itself (derived). The first test of the effort should measure a 1 to 3 mm thick insert with perpendicular fiber at a fixed fiber fraction, with the plated face attached, in a thermal-cycling and hot water-glycol exposure.

1. Introduction and Scope

The CF-JET proposal places a printed carbon fiber target plate between a heat source and a jet-impingement coolant path. The plate has a light, low-expansion body, an insert or region where heat crosses the plate thickness, and a sealed face that the coolant jets strike. Figure 1 shows the concept and the points where this paper tests the proposal claims.[14]

Figure 1. Operational concept of the CF-JET target plate and scope of the paper

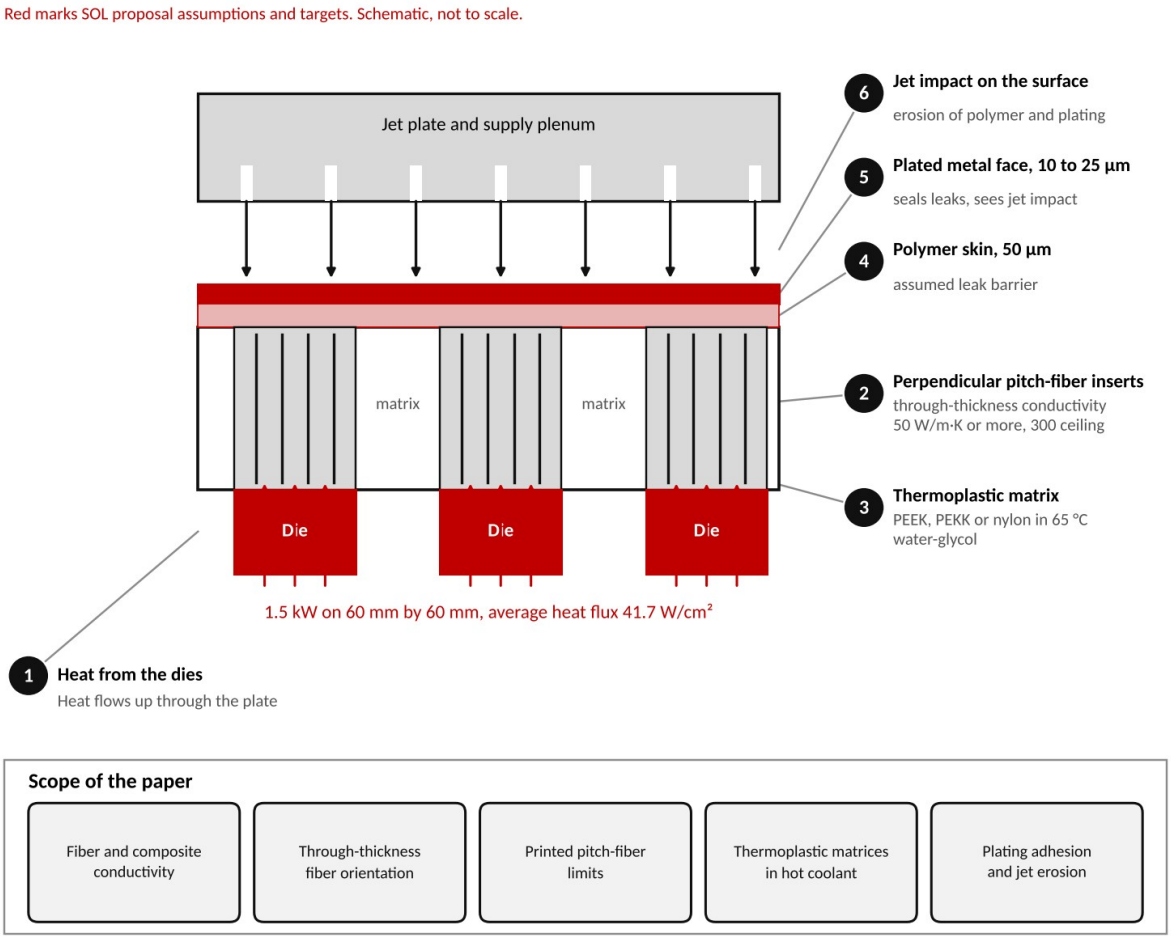

The operating conditions, geometry and insert thickness are SOL proposal assumptions or assumptions of this paper.[15] *The diagram is schematic and not to scale.*

The design point is 1.5 kW on a 60 mm by 60 mm footprint, which is 36 cm² and an average heat flux of 41.7 W/cm², with 50/50 water-glycol entering at 65 °C at 4 to 8 L/min, a pressure drop of 30 kPa or less and a case-to-coolant resistance of 0.02 K/W.[16] The resistance equals 72 mm²·K/W on the footprint (derived), and at 41.7 W/cm² it corresponds to a temperature difference of 30 K across the whole stack (derived). Every layer between the case and the coolant draws on that budget.

The scope covers six topics. The first is the axial and transverse thermal conductivity of pitch-based and PAN-based fibers and the documented composite-level through-thickness values. The second is the set of processes that produce through-thickness fiber orientation and the fiber volume fraction each one achieves. The third is whether continuous carbon fiber printers can process pitch fiber, and what consolidation and void limits apply. The fourth is the behavior of PEEK, PEKK and nylon in hot water-glycol. The fifth is plating adhesion on carbon fiber composites under thermal cycling. The sixth is erosion of polymer surfaces under liquid jet impact. The paper closes with a test of six proposal claims, listed in Table 9 with their verdicts.

2. Fiber and Composite Conductivity

2.1 Pitch fiber conducts 140 to 1,000 W/m·K along the axis, and measured values fall under the vendor values

Axial conductivity in carbon fiber follows the degree of graphitic alignment, which also sets the tensile modulus. Mitsubishi Chemical lists K13D2U at 800 W/m·K and 935 GPa with a coefficient of thermal expansion of −1.3 ppm/K, against 1,950 W/m·K for a graphite crystal and 400 W/m·K for copper.[17] A thesis at York University measured three K13D2U tows at 768, 792 and 775 W/m·K, an average of 778 W/m·K, which is 97 percent of the vendor value (derived).[18] The same thesis reports a manufacturer density of 2.20 g/cm³ and a measured density of 2.1682 g/cm³, with 2,000 filaments of 10.58 µm mean diameter per tow.[19]

K1100 shows the temperature dependence that matters at the 65 °C coolant condition. A measurement at the Pacific Northwest National Laboratory gave 576 W/m·K at 27 °C, falling to 242 W/m·K at 1,000 °C, and a laboratory presentation lists 1,000 W/m·K for the same fiber, so the measured value is 58 percent of the listed value (derived).[2021] Lower-modulus pitch fibers conduct less: Nippon Graphite lists 500 W/m·K for XN-90 at 860 GPa, 320 W/m·K for XN-80 and 600 W/m·K for HC-600, and NASA lists 200 and 320 W/m·K for the YSH-60A and YSH-80A fibers.[2223] A target of 50 W/m·K at under 9 percent fiber needs a fiber near 800 W/m·K, which selects the top of the pitch range, and the supplier value is a ceiling for the tow value.

Table 1. **Fiber thermal conductivity along the axis**

Fiber	Precursor	Axial k (W/m·K)	Other reported properties	Evidence
K1100	Pitch	576 at 27 °C; 242 at 1,000 °C; 1,000 listed	Density 2.20 g/cm³ (listed)[2425]	Measured; laboratory presentation
K13D2U	Pitch	800 listed; 768, 792, 775 measured on tows	935 GPa; CTE −1.3 ppm/K; 3.70 GPa strength[2627]	Vendor; measured
XN-90	Pitch	500 listed	860 GPa[28]	Vendor
XN-80 and HC-600	Pitch	320 and 600 listed	Grade chart[29]	Vendor
YSH-60A and YSH-80A	Pitch	200 and 320 listed	634 and 786 GPa[30]	Government report; vendor values
P55 and P120	Pitch	120 and 640 listed	2.00 and 2.17 g/cm³[31]	Government laboratory presentation
HR40	PAN	65.2 ± 2.6 measured	Single fiber, lock-in thermography[32]	Peer-reviewed; measured
HTS40	PAN	8.8 ± 0.7 measured	Single fiber[33]	Peer-reviewed; measured
PAN high modulus and high tenacity	PAN	70 and 10 listed	Grade chart[34]	Vendor
Ultra-high-modulus and standard-modulus	Not stated	Up to 200 and 9 to 11 listed	Marketing information[35]	Vendor

Vendor and presentation values are listed values. The K13D2U density measurement and the tow conductivities come from a thesis and are not independent of the vendor product. Values are as reported and no conversion was applied.

Figure 2. **Fiber and composite conductivity on a logarithmic scale against the CF-JET targets**

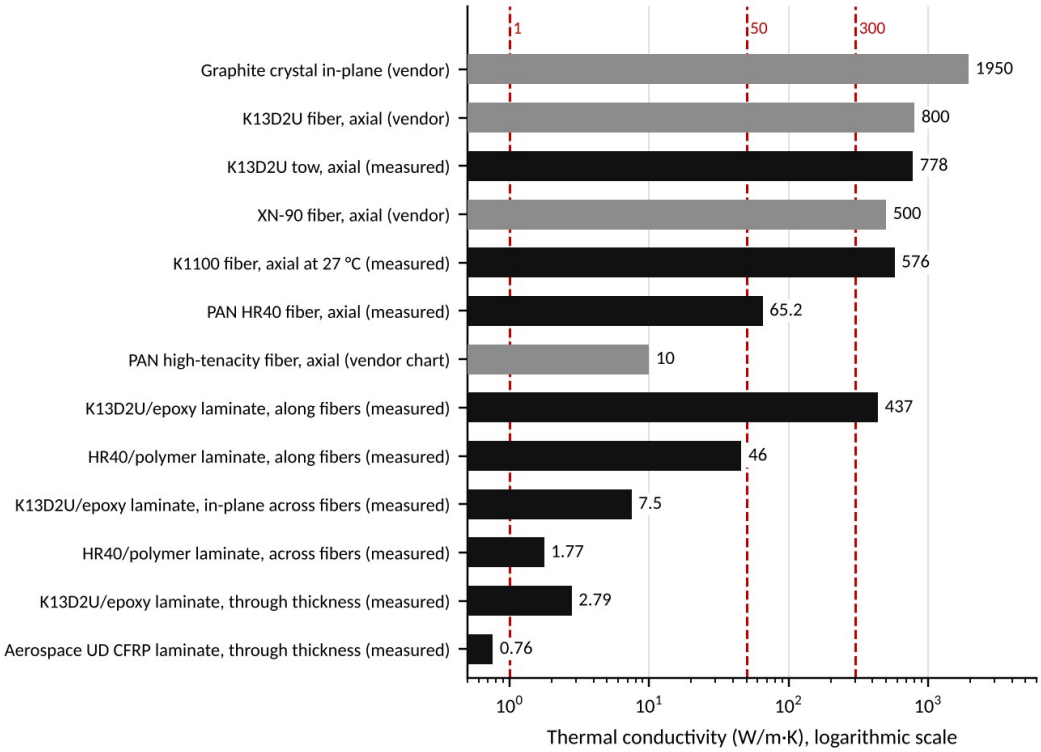

Black: measured or reported values. Grey: manufacturer or vendor values. Red dashed lines: values in the CF-JET claims.

Black bars are measured values. Grey bars are vendor or listed values. Red dashed lines mark 1 W/m·K (the claimed printed through-thickness value), 50 W/m·K and 300 W/m·K (the claimed insert target and ceiling).

2.2 Conductivity across the fiber is 3 to 21 percent of the axial value in the PAN fibers measured

The through-thickness conduction of an ordinary laminate is set by the transverse conductivity of the fiber and the resin. Bard et al. measured single PAN fibers with lock-in thermography and composites with laser flash. The HR40 fiber has an axial conductivity of 65.2 W/m·K, and an HR40 composite at 65 volume percent has an axial value of 46 W/m·K and a transverse value of 1.77 W/m·K, a ratio of 26 (derived).[36] The authors cite a general figure of about 1 percent for transverse over longitudinal conductivity.[37] The anisotropy ratio rises with fiber modulus: the paper reports ratios of 4.8, 8.3 and 8.5 for three lower-modulus fibers and 29.4 ± 2.6 for HR40.[38]

The transverse value also governs what a high-conductivity fiber adds when it lies in the plane. For K13D2U laminates measured at Purdue, the conductivity across the fibers in the plane is 7.5 ± 4.4 W/m·K and the through-thickness value is 1.39 to 1.44 W/m·K at 4 to 7 bar consolidation, against 376 to 437 W/m·K along the fibers.[39] The in-plane axial value is 260 to 315 times the through-thickness value (derived), and a laminate with its fibers in the plane gains almost nothing through the thickness from the fiber conductivity.

2.3 Laminates of pitch fiber conduct 0.76 to 2.8 W/m·K through the thickness

Table 2 lists the through-thickness values retrieved for carbon fiber composites. A unidirectional laminate at 57 percent fiber measured 0.894 ± 0.160, 0.770 ± 0.049 and 0.758 ± 0.040 W/m·K at three thicknesses by guarded hot plate, with an interface conductance of 1,100 W/m²K.[40] The Purdue measurements on

K13D2U with EX1515 resin reach 1.39 to 1.44 W/m·K at 51.6 percent fiber and 2.79 ± 0.46 W/m·K at 74.5 percent, and a cross-ply layup reaches 4.0 ± 0.6 W/m·K at 20 bar.[41] The NASA study of hybrid PAN and pitch architectures reports a baseline of 0.974 to 0.984 W/m·K, and the percentage gains it reports for pitch fiber give 1.14 to 1.45 W/m·K (derived from reported percentages).[42]

These values support the claim that a printed carbon fiber plate conducts about 1 W/m·K or less through its thickness for layups with fibers in the plane at moderate fiber fractions. They exceed 1 W/m·K for laminates with pitch fiber at 52 to 75 percent fiber, with a range of 1.2 to 4.0 W/m·K across the cases in Table 2. No through-thickness measurement of a printed carbon fiber part was found. Printing creates voids and wide spacing between rasters, so the laminate values are an upper reference and the printed value is unmeasured.

Table 2. Through-thickness thermal conductivity of carbon fiber composites

Material	Fiber fraction	Through-thickness k (W/m·K)	Method	Evidence
Unidirectional CFRP, three thicknesses[43]	57%	0.894 ± 0.160; 0.770 ± 0.049; 0.758 ± 0.040	Guarded hot plate	Conference paper; measured
K13D2U in EX1515, unidirectional[44]	51.6% at 4 bar; 74.5% at 20 bar	1.44 ± 0.24 at 4 bar; 1.39 ± 0.10 at 7 bar; 2.79 ± 0.46 at 20 bar	Laboratory measurement	Web report; measured
K13D2U in EX1515, cross-ply[45]	Not stated	1.36 and 1.5; 4.0 ± 0.6 at 20 bar	Laboratory measurement	Web report; measured
K13C2U in EX1515, unidirectional[46]	Not stated	1.18 ± 0.15 (the page also lists 1.09), 1.36 and 2.21	Laboratory measurement	Web report; measured
AS4 in epoxy, control[47]	About 76%	1.31	Steady-state parallel plate	Peer-reviewed; measured
AS4 in epoxy with unaligned nanofiber[48]	Not stated	3.61	Steady-state parallel plate	Peer-reviewed; measured
AS4 in epoxy with nanofiber z-threads[49]	About 72%	9.85	Steady-state parallel plate	Peer-reviewed; measured
PAN braid baseline and pitch-hybrid braids[50]	57% average	0.974 to 0.984 baseline; 1.14 to 1.45 with pitch (derived)	Steady-state between references	Government report; measured and derived
Chopped AS4 in epoxy, rotational direct ink writing[51]	7.9%	0.292 at 0 rpm; 0.409 at 876 rpm	Laser flash	Peer-reviewed; measured

The derived values for the NASA hybrids multiply the reported baseline by the reported percentage change, so they are approximate. The Purdue page does not explain the two K13C2U values for one case. Fiber fractions of the Purdue cases correspond to the pressure shown where the page states them.

2.4 A parallel-conduction estimate sets the fiber fraction needed for the insert targets

For heat flowing along the fiber, the composite conductivity is the sum of the fiber and matrix contributions weighted by volume: k = Vf·kf + (1 − Vf)·km. With kf = 800 W/m·K and a PEEK matrix of 0.29 W/m·K, an insert conductivity of 50 W/m·K needs a fiber fraction of 6.2 percent, and 300 W/m·K needs 37.5 percent (derived).[52] Fibers that are less than perfectly straight or less than fully connected reduce the contribution, and a 70 percent efficiency raises the requirement to 8.9 and 53.5 percent (derived, Table 3). A 500 W/m·K fiber needs 9.9 and 60.0 percent, and a 600 W/m·K fiber needs 50.0 percent for the 300 W/m·K ceiling (derived).

Table 3. Perpendicular fiber volume fraction needed for the insert conductivity targets (derived)

Fiber and efficiency	kf (W/m·K)	50 W/m·K target	100 W/m·K	300 W/m·K ceiling
K13D2U-class fiber, ideal alignment	800	6.2%	12.5%	37.5%
K13D2U-class fiber, 70% efficiency	560 effective	8.9%	17.8%	53.5%
High-modulus pitch fiber, ideal alignment	600	8.3%	16.6%	50.0%
Mid-range pitch fiber, ideal alignment	500	9.9%	20.0%	60.0%

Derived from k = Vf·kf + (1 − Vf)·km with km = 0.29 W/m·K. The 70 percent efficiency is an illustrative assumption and is not a measured value. The 100 W/m·K column is added for reference.

Figure 3. Conductivity along the fibers against fiber volume fraction, with printed and aligned measurements

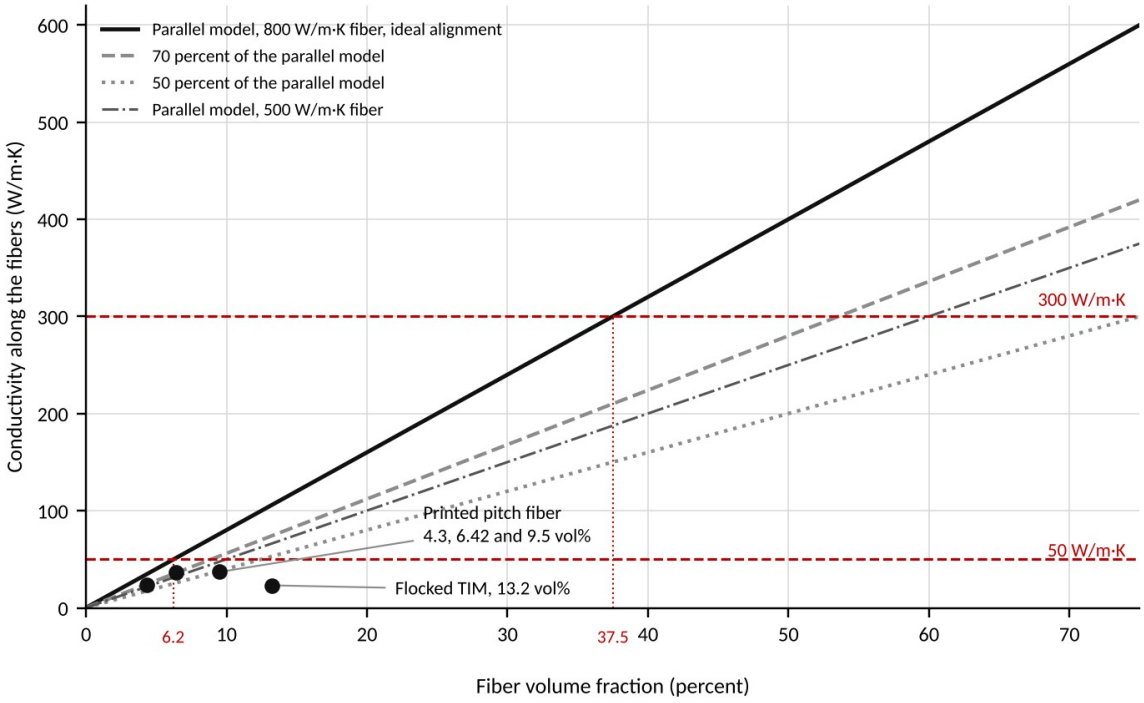

Lines are parallel-conduction estimates for the fiber conductivities shown. Printed points are from York University work and a cited earlier study; the Ibrahim point is plotted against an assumed 800 W/m·K fiber and was not read in the original.[535455]

The printed measurements fall under the parallel estimate. A printed sample at 6.42 percent fiber measured 36.63 W/m·K, which is 0.71 of the estimate for an 800 W/m·K fiber (derived).[56] A printed sample at 9.5 percent measured 37.1 W/m·K, 0.49 of the estimate (derived), and the authors report it as 50 to 65 percent under the parallel model.[57] A sample at 4.3 percent measured 23.6 W/m·K, 0.68 of the estimate against an assumed 800 W/m·K fiber (derived).[58] At 50 W/m·K the printed route needs between 6.2 and 8.9 percent fiber if the efficiency matches the best printed value, which is near the reported 6.42 percent ceiling.

2.5 Composite density and expansion depend on the fiber fraction

A rule of mixtures with a 2.17 to 2.20 g/cm³ pitch fiber and a 1.30 g/cm³ PEEK matrix gives 1.36 g/cm³ at 6.42 percent fiber, 1.56 to 1.57 at 30 percent, 1.735 to 1.75 at 50 percent, 1.78 to 1.80 at 55 percent and 1.82 to 1.84 at 60 percent (derived).[5960] The claimed composite density of 1.5 to 1.8 g/cm³ holds from

about 23 to 55 percent fiber for pitch fiber in PEEK (derived), and a plate with a 6 to 9 percent insert region lies under 1.5 g/cm³ in that region. A PAN fiber density was not retrieved.

Along the fiber, the axial expansion of K13D2U is −1.3 ppm/K, and a matrix of 55 ppm/K under the glass transition governs the composite at low fiber fractions.[6162] With an assumed matrix modulus of 3.6 GPa, which is an assumption and not a sourced value, the composite expansion along the fibers is 7.6 ppm/K at 2 percent fiber, 3.46 at 4 percent, 1.69 at 6.42 percent, 0.59 at 10 percent and −0.45 ppm/K at 20 percent (derived). The claimed 0 to 4 ppm/K therefore holds along the fibers for fiber fractions of 3.6 percent or more, and reaches 0 at 14 percent. Across the fibers the expansion follows the matrix and fiber packing, and a PEEK matrix expands 45 to 55 ppm/K under the glass transition.[63] In an insert region with fibers perpendicular to the plate, the in-plane direction is the transverse direction, so the 0 to 4 ppm/K claim describes the fibers in the plate plane and does not describe the insert region.

3. Processes That Produce Through-Thickness Fiber Orientation

3.1 Aligned fiber thermal interface materials reach 15 to 52 W/m·K at thicknesses under a few millimeters

The highest through-plane values for carbon fiber composites come from interface materials in which pitch fibers stand perpendicular to the sheet. Electrostatic flocking of mesophase pitch fiber gave 15.3 W/m·K at 13.4 weight percent, which is 60.2 times the matrix.[64] A later flocking study reports 24.47 W/m·K at 6.30 weight percent and 28.97 W/m·K with 2 percent carbon nanotubes, and cites an earlier value of 23.3 W/m·K at 13.2 volume percent.[65] Direct ink writing of aligned fiber followed by slicing perpendicular to the fiber gave 35.22 W/m·K, which is 1,213 times the PDMS matrix, and a 17.4 °C lower temperature than a commercial interface material in a test device.[66] A rolling-press process reached 51.90 W/m·K at 73.68 weight percent filler, 323 times the PDMS matrix, and a total resistance that fell from 0.55 to 0.32 K·cm²/W (32 mm²·K/W) after surface modification.[67]

These values come from soft elastomer matrices and thin sheets. The 32 mm²·K/W total resistance includes contact resistance at both faces, and it equals 44 percent of the 72 mm²·K/W budget before any other layer is counted (derived). No measurement of a 1 to 3 mm thick insert with perpendicular fiber in a thermoplastic matrix was found, and the second case reports fiber as weight percent, while the fiber content of the first case was not retrieved.

Table 4. Processes for through-thickness fiber orientation and reported conductivity

Process	Mechanism	Reported through-thickness k (W/m·K)	Fiber content	Evidence and limit
Sliced aligned block[6869]	Fibers aligned by printing or rolling, then cut perpendicular to the fiber	35.22; 51.90	51.90 at 73.68 wt%; first case not retrieved	Peer-reviewed; PDMS matrix, thin sheet
Electrostatic flocking[7071]	Short fibers stand in an electric field, resin fills the array	15.3; 23.3 (cited); 24.47; 28.97 with 2% nanotubes	13.4 wt%; 13.2 vol%; 6.30 wt%	Peer-reviewed; thin interface layer
Pultruded rod and z-pin[7273]	Rods inserted through the laminate thickness	Not reported; electrical resistance fell by two orders of magnitude at 0.1 and 0.25 vol% pins	0.1 to 0.25 vol%	Peer-reviewed for electrical data; patent for thermal use

Process	Mechanism	Reported through-thickness k (W/m·K)	Fiber content	Evidence and limit
Carbon nanofiber z-thread[74]	Flow-aligned nanofiber threads between plies	9.85	About 72% carbon fiber; thread loading limited to 1 wt%	Peer-reviewed; measured
Rotational direct ink writing[75]	Nozzle rotation tilts chopped fiber	0.409 at 876 rpm, 40% over the unrotated value	7.9 vol% of 300 µm fibers	Peer-reviewed; low conductivity
Pitch fiber hybrid braid[76]	Co-braided pitch tows with PAN	1.14 to 1.45 (derived)	About 50% pitch within 57% total fiber	Government report; fibers not perpendicular

The sliced-block and flocking values apply to thin interface sheets in elastomer or epoxy matrices. No row reports a millimeter-thick insert in a thermoplastic matrix.

3.2 Z-pins and pultruded rods have thermal use cases and electrical data

Z-pins are small pultruded rods inserted through a laminate before cure. Chen et al. used T300 and bismaleimide pins and copper pins at 0.1 and 0.25 volume percent, and the pins cut the through-thickness electrical resistance by two orders of magnitude with a much smaller data variation.[77] The measurement is electrical. A Lockheed Martin patent describes z-pins for through-thickness heat conduction.[78] A conductivity estimate for pitch fiber pins uses the same parallel relation as Table 3: pins of K13D2U-class fiber at 6.2 percent would raise a plate to 50 W/m·K if every pin spanned the thickness without a gap, and pins at 0.25 percent contribute 2.3 W/m·K (derived).

The fiber fraction a pin array reaches is limited by the pin diameter and the damage the pin makes in the laminate. The values reported for pins are 0.1 to 0.25 volume percent, and the electrical study cited a literature range of 0.2 to 4 percent for other pin materials.[79] At 4 percent the pitch fiber estimate is 32 W/m·K at full efficiency (derived), under the 50 W/m·K claim. A pitch fiber rod fails at about 0.4 percent strain (derived), so rods must stay straight during placement.

3.3 Sliced unidirectional blocks reach the highest fiber content and have no thick-insert data

A pultruded or wound block of unidirectional pitch fiber at 55 to 70 percent fiber could be sliced across the fibers into plugs of the insert thickness. In the sliced interface materials, fiber content reaches 73.68 weight percent, and the unidirectional K13D2U laminates at Purdue reach 74.5 percent by volume at 20 bar.[8081] At 55 percent and 800 W/m·K, the parallel estimate is 440 W/m·K, and at 70 percent efficiency 308 W/m·K (derived). The route reaches the 300 W/m·K ceiling only with the sliced-block fiber fraction and not with the 6 to 9 percent fraction of printed inserts. Cutting and bonding of 1 to 3 mm plugs into a printed plate is a joining problem that no source in this review addresses, and the plug-to-plate interface adds resistance at both faces.

4. Printed Continuous Pitch Fiber and Its Limits

4.1 Pitch fiber breaks at a bend radius of about 1.3 mm

Pitch fiber is stiff and brittle. K13D2U has a tensile modulus of 935 GPa and a strength of 3.70 GPa, so its failure strain is 0.396 percent (derived).[8283] A filament of 10.58 µm diameter fails when bent to a radius of about 1.34 mm, and at 11 µm the radius is 1.39 mm (derived from $\varepsilon = d/2R$). A printer that turns the fiber through a right-angle nozzle exit applies a smaller radius than this to the filament surface, and the York

work found breakage sources at the nozzle angle, in drag, and at speeds over about 2,500 mm/min.[84] A 6-axis robot study with an angled nozzle and PLA-coated fiber found that a right-angle exit breaks pitch fiber, that shallower extrusion angles gave effective conductivities up to 82 percent of the specified fiber value, and that curved paths under 30 mm radius and sharp corners reduced conductivity.[85]

The York thesis improved a hand-laid sample with pause-at-layer deposition to 36.63 ± 1 W/m·K at 6.42 percent fiber, about 30 percent under the parallel estimate, with PLA-coated fiber and PLA-coated tows that retained most of their tow conductivity.[86] A 10° print angle nearly eliminated breakage with a new extruder, and the baseline speed was 800 mm/min.[87] The thesis reports 6.42 percent as the practical ceiling. The thesis abstract describes a full-scale printed composite sample, and the thesis text read places full-scale printing outside its scope, so the construction of the 36.63 W/m·K sample should be confirmed with the authors before it is used as a printed-part benchmark. Void content was not reported.[88]

4.2 No documentation of commercial continuous fiber printers processing pitch fiber was found

The published pitch fiber prints come from laboratory printers: a custom dual-nozzle extruder that measured 37.1 W/m·K effective conductivity and found fiber breaking during the process, and a 6-axis robot arm.[8990] A search for pitch fiber compatibility in commercial printer documentation returned no result, which is an evidence gap. The commercial printer data that exist concern other fibers. Parker et al. found that printing reduced ultimate tensile strength by 8 to 62 percent across Toray T-40 and T-50 filaments and the Markforged filament on a modified Prusa and a Mark Two, with no correlation between strength loss and fiber fraction.[91] The damage came from extruder roller contact, nozzle passage and deposition, and the authors identify deposition, with bending of peripheral fibers and contact with the nozzle rim, as the most damaging stage.[92] A pitch fiber, with a failure strain a quarter of the value for standard-modulus fibers, is more sensitive to all three stages (derived from the failure strains in this paper and the strength of the standard fibers, which was not retrieved).

4.3 Printed composites hold about 12 percent voids unless consolidated again

A study on a Markforged Mark Two reports a typical void content of about 12 percent for printed composites, with a fiber fraction that is low, 28.8 percent in the sample tested.[93] Compression at 5 bar and 280 °C for 20 minutes cut the void content from 12.2 to 1.8 percent and left the fiber fraction at 28.8 percent.[94] The matrix in that study is a carbon fiber-filled polyamide, so the result establishes the size of the void problem for printed composites and a consolidation route, and it was not measured on PEEK or on pitch fiber. A printed plate with a sealed face needs a void-free surface layer, because voids that connect to the coolant face would leak. Table 5 collects the printed pitch fiber results and the void and consolidation findings.

Table 5. Printed continuous fiber results, breakage limits and void content

Study	Fiber and process	Result	Limit reported	Evidence
Olcun et al., 2023[9596]	Pitch fiber, custom dual-nozzle printer	37.1 W/m·K at 9.5 vol%; 50 to 65% under the parallel model	Fiber breakage confirmed by imaging and computed tomography	Peer-reviewed; measured
Ibrahim et al.[97]	Continuous fiber, printed	23.6 W/m·K at 4.3 vol%	Not read in the original	Cited; measured

Study	Fiber and process	Result	Limit reported	Evidence
Ali, 2026[98]	Pitch fiber, PLA-coated, pause-at-layer	36.63 ± 1 W/m·K at 6.42 vol%; about 30% under the parallel model	Practical ceiling 6.42 vol%; breakage over about 2,500 mm/min; 10° print angle nearly eliminated breakage	Thesis; measured
Olcun et al., 2024[99]	Pitch fiber, 6-axis robot, angled nozzle	Effective fiber conductivity up to 82% of specified	Radius under 30 mm and sharp corners reduce conductivity	Peer-reviewed; measured
Parker et al., 2023[100]	Carbon filaments, modified Prusa and Mark Two	Strength loss of 8% to 62% from printing	Roller, nozzle and deposition damage; no link to fiber fraction	Peer-reviewed; measured
Yudhanto et al., 2023[101]	Markforged Mark Two, carbon fiber in polyamide	Void content 12.2% before and 1.8% after compression	Fiber fraction 28.8%; polyamide matrix	Peer-reviewed; measured

The Ibrahim et al. value was read in a citing paper and is not confirmed in the original. The Yudhanto matrix is a carbon fiber-filled polyamide and the result is not a pitch fiber measurement.

5. Thermoplastic Matrices in Hot Water-Glycol

5.1 PEEK showed no mass change in 90 days of hot water at 120 to 160 °C, and no glycol data were found

PEEK 450G has a glass transition onset of 143 °C, a thermal conductivity of 0.29 W/m·K on average and 0.32 W/m·K along the flow direction at 23 °C, a density of 1.30 g/cm^3, a melting point of 343 °C and a water absorption at saturation of 0.45 percent at 23 °C and 0.55 percent at 100 °C.[102] The coolant inlet of 65 °C lies 78 K under the glass transition onset (derived). Porto et al. aged PEEK for 90 days at 120, 140 and 160 °C in air, in water bubbled with nitrogen, in water bubbled with air and in water at pH 4. Density measurements showed no water absorption or mass loss, the onset of thermal degradation varied by under 5 °C from unaged material, and Young's modulus changed little.[103] Tensile strength and elongation at rupture changed more, most strongly in the air-saturated water and the acidic solution.[104] The study used water without glycol, and it reports no numerical tensile changes in the text read, so the glycol effect and the size of the strength change remain open.

5.2 PEKK has a higher glass transition and a 70 °C record of 30 days

PEKK has a glass transition of 156 to 165 °C against 143 °C for PEEK.[105] A carbon fabric and PEKK laminate in a 70 °C wet condition took up about 0.27 weight percent moisture and kept 90.0 and 89.3 percent of its warp and weft bending strength, 97.7 and 97.3 percent of its bending modulus, about 90 percent of its in-plane shear strength and about 85.8 percent of its interlaminar shear strength, which was the largest reduction among the properties tested.[106] A carbon fiber and PEKK laminate made by automated fiber placement with 5 percent voids lost 6.5 percent of its tensile strength, 5.2 percent of its failure strain and 4 percent of its modulus after 30 days in 70 °C water, and infrared, calorimetry and dynamic mechanical tests showed plasticization, post-crystallization and a second glass transition.[107] Both studies used water at 70 °C and no glycol, and the 70 °C condition is 5 K over the CF-JET inlet. No PEKK data in water-glycol at 65 °C or higher were found, which is an evidence gap.

5.3 Nylon 66 loses molar mass in hot water-glycol and plasticizes, and the data begin at 120 °C for the polymer

Laügt et al. aged injection-molded nylon 66 in a water and ethylene glycol antifreeze fluid at 120 to 140 °C for 48 to 1,000 hours. Molar mass fell by up to 65 percent after 336 hours at 140 °C and by about 34 percent after 336 hours at 120 °C, and the glass transition of the amorphous phase, which governs stiffness at room temperature, fell from about 70 °C to between −22 and −17 °C from plasticization.[108] The modulus stayed roughly stable at 780 to 1,030 MPa, and the loss of molar mass embrittled the polymer.[109] The authors conclude that fluid intake plasticizes the material, that molar mass loss embrittles it, and that crystalline changes affect stiffness.[110]

Glass fiber reinforced nylon 66 in water-glycol mixtures was characterized at 70, 120 and 150 °C for up to 1,000 hours, and the mechanical performance at the different temperatures superimposed when plotted against the amount of fluid absorbed by the matrix.[111] A swelling study covered 50 and 70 °C for up to 900 hours in water, ethylene glycol and an antifreeze mixture.[112] The 65 °C CF-JET condition lies between the lowest tests of the two studies, so the loss rate at 65 °C requires extrapolation from tests at 70 °C and higher, and the strength of a carbon fiber nylon laminate was not measured in any of these sources. Table 6 sets the three matrices side by side.

Table 6. Thermoplastic matrix evidence in hot water and water-glycol

Matrix	Glass transition	Hot-liquid evidence	Condition tested	Evidence
PEEK 450G[113][114]	143 °C onset	No water uptake or mass loss; tensile strength and elongation changed most in air-saturated and acidic water; modulus changed little	Water, 120 to 160 °C, 90 days; no glycol	Vendor; peer-reviewed
PEKK (carbon fabric laminate)[115]	156 to 165 °C	0.27 wt% moisture; bending strength retained 90%; interlaminar shear strength retained 85.8%	Wet, 70 °C; no glycol	Peer-reviewed
PEKK (carbon fiber laminate, 5% voids)[116]	Second glass transition formed	Tensile strength −6.5%; failure strain −5.2%; modulus −4%	Water, 70 °C, 30 days; no glycol	Peer-reviewed
Nylon 66[117]	Amorphous-phase transition fell from about 70 °C to between −22 and −17 °C	Molar mass −65% at 140 °C and −34% at 120 °C after 336 h; modulus stable at 780 to 1,030 MPa	Water-ethylene glycol, 120 to 140 °C, 48 to 1,000 h	Peer-reviewed
Glass fiber nylon 66[118][119]	Not stated	Performance superimposes against absorbed fluid; swelling measured	Water-glycol, 70 to 150 °C up to 1,000 h; 50 and 70 °C up to 900 h	Conference paper; peer-reviewed

The CF-JET fluid is 50/50 water-glycol at 65 °C.[120] Rows with water only do not establish glycol behavior, and rows at 70 °C or higher require extrapolation to 65 °C.

6. Plated Face, Skin and Interface Resistance

6.1 Plating adhesion has scratch-test and pull-off data and no record of cycling in hot glycol

Gao et al. deposited electroless Ni-P on PEEK, carbon fiber filled PEEK (CF30/PEEK) and glass fiber filled PEEK (GF30/PEEK), with the best adhesion at a surface roughness of 0.4 µm, and found that the fiber-reinforced PEEK adhered better than neat PEEK.[121] The only numerical adhesion value in the paper is 4.2 N for CF30/PEEK at a roughness of 0.2 µm by scratch test, and the coating was 13.9 µm thick.[122] The study applied no thermal cycling.[123] Integran patents describe nanocrystalline Ni-Fe or Ni coatings of 20 to 250 µm on graphite and epoxy, carbon fiber and bismaleimide, and carbon fiber and epoxy substrates, with

pull-off adhesion of 350 to 1,069 psi (2.4 to 7.4 MPa, derived), ten cycles from 85 to −40 °C under ASTM B604 with about 0 percent displacement, and thirty cycles from −196 to 90 °C without failure.[124] The patents give a substrate expansion of 5 ppm/K in the plane and 55 to 60 ppm/K normal to the plane for graphite and epoxy.[125]

The evidence covers the metals and substrates but not the CF-JET condition. The thermal cycles in the patents stop at 90 °C and take place in air, and the plated face in CF-JET sees water-glycol at 65 °C with jets on the metal. A 55 to 60 ppm/K normal expansion of the substrate acts against a metal layer, and an insert with perpendicular fiber changes the local expansion pattern in a way that no source measured. No peer-reviewed plating adhesion data under thermal cycling in hot water-glycol for carbon fiber and thermoplastic stacks was found. The adhesion requirement can be stated from the test conditions: cycles between the dry condition and the 65 °C wetted condition, with pull-off tests before and after, on the final plate construction.

6.2 A copper layer of 10 to 25 µm adds under 0.1 percent of the budget, and a polymer skin does not

The resistance of a layer is its thickness over its conductivity. Copper at 400 W/m·K gives 0.025 mm²·K/W for 10 µm and 0.0625 mm²·K/W for 25 µm, which are 0.03 and 0.09 percent of the 72 mm²·K/W budget (derived).[126] Electroless Ni-P conducts less. One source states that the alloy at 12.7 weight percent phosphorus has about half the conductivity of pure nickel.[127] An illustrative bounding value of 5 W/m·K, an assumption chosen as a low case and not a sourced value, gives 2.0 and 5.0 mm²·K/W for 10 and 25 µm, or 2.8 and 6.9 percent of the budget (derived). The claim that a 10 to 25 µm plated layer adds negligible resistance therefore holds for copper and is a bounded case for Ni-P.

A polymer skin changes the result. At 50 µm and 0.25 W/m·K the resistance is 0.0556 K/W, which is 200 mm²·K/W on 36 cm² and 2.78 times the whole 0.02 K/W budget (derived). The claimed 0.056 K/W therefore follows from a conductivity of 0.248 W/m·K, and the arithmetic holds. At PEEK conductivities of 0.29 and 0.32 W/m·K the skin gives 0.0479 and 0.0434 K/W, which are 172 and 156 mm²·K/W (derived).[128] A skin that uses half of the budget is about 10.4 µm thick at 0.29 W/m·K, and a skin that uses 10 percent is about 2.1 µm thick (derived). At 41.7 W/cm² a 172 mm²·K/W skin produces a temperature difference of 72 K (derived), against 30 K for the whole budget, so the jet-side face must be a plated or conductive layer.

6.3 Insert thickness and conductivity set the conduction share of the budget

Table 7 gives the conduction resistance 1000·t/k of an insert of 1, 2 and 3 mm at the conductivities reported in Table 4 and Table 5, and at 100 and 300 W/m·K as references. The insert thicknesses are assumptions of this paper, since no target plate geometry was available. A 1 mm insert at 51.9 W/m·K uses 19.3 mm²·K/W, which is 27 percent of the budget, and a 2 mm printed insert at 36.6 W/m·K uses 54.6 mm²·K/W, which is 76 percent (derived). The 300 W/m·K ceiling at 1 mm uses 3.3 mm²·K/W, 5 percent of the budget.

Table 7. Conduction resistance of a perpendicular-fiber insert by thickness (derived)

k (W/m·K)	Basis	1 mm (mm²·K/W)	2 mm (mm²·K/W)	3 mm (mm²·K/W)
15.3	Flocked pitch fiber interface material[129]	65.4	130.7	196.1
23.3	Flocked pitch fiber, cited earlier value[130]	42.9	85.8	128.8
35.2	Printed-aligned and sliced interface material[131]	28.4	56.8	85.2

k (W/m·K)	Basis	1 mm (mm²·K/W)	2 mm (mm²·K/W)	3 mm (mm²·K/W)
36.6	Printed pitch fiber at 6.42 vol%[132]	27.3	54.6	81.9
51.9	Rolling-press interface material[133]	19.3	38.5	57.8
100	Reference value	10.0	20.0	30.0
300	Claimed ceiling[134]	3.3	6.7	10.0

The budget is 72 mm²·K/W on 36 cm². The values equal 1000·t/k with the thickness t in millimeters and are not measured values. They exclude convection, spreading, contact and skin resistance.

Figure 4. Insert resistance against conductivity for 1, 2 and 3 mm thicknesses with the CF-JET budget

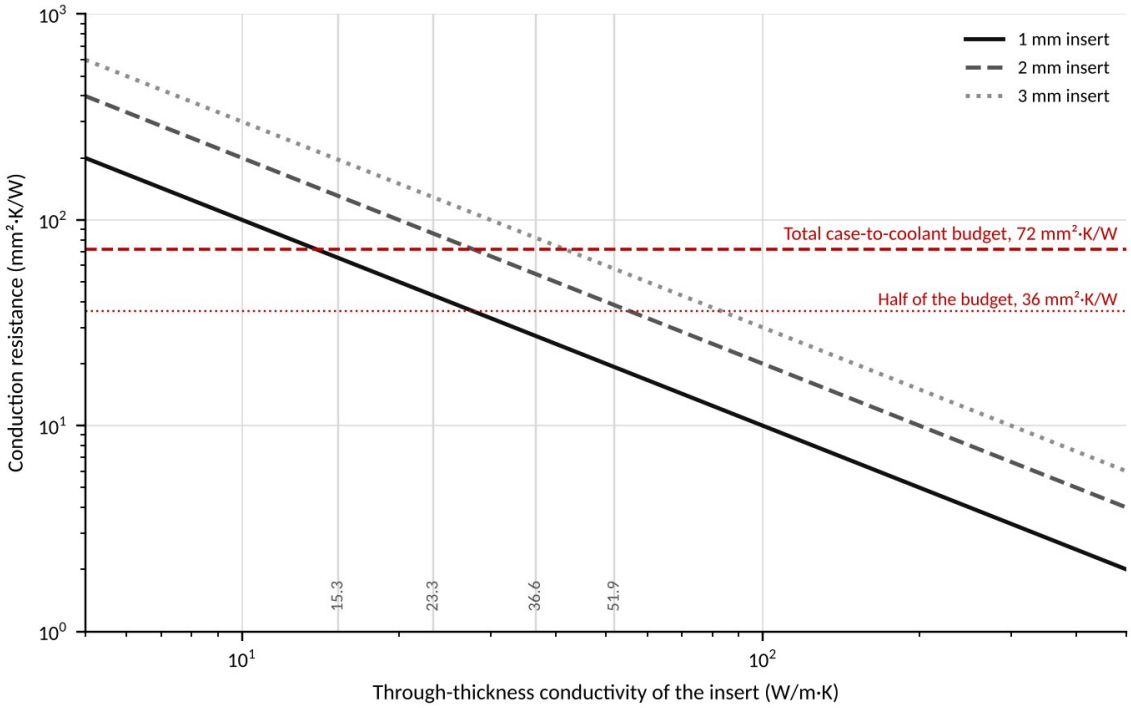

Derived from resistance equal to thickness over conductivity. The insert thicknesses are assumptions. The 72 mm²·K/W line is the 0.02 K/W target on 36 cm², and the 36 mm²·K/W line is half of that budget.[135]

Figure 5 combines the layers for five illustrative builds. Build A, a 1 mm insert at 51.9 W/m·K with a copper face, totals 19.4 mm²·K/W. Build B, a 2 mm printed insert at 36.6 W/m·K with copper, totals 54.7. Build C, a 1 mm insert at 300 W/m·K with a 10 µm polymer skin and copper, totals 37.9 and is dominated by the skin at 34.5. Build D, a 1 mm insert at 51.9 W/m·K under a 50 µm skin, totals 191.8, and Build E, the 2 mm printed insert under the same skin, totals 227.1 (derived). Builds D and E exceed the budget by 2.7 and 3.2 times before any convective resistance is counted.

Figure 5. Conduction resistance of five illustrative target plate builds against the 72 mm²·K/W budget

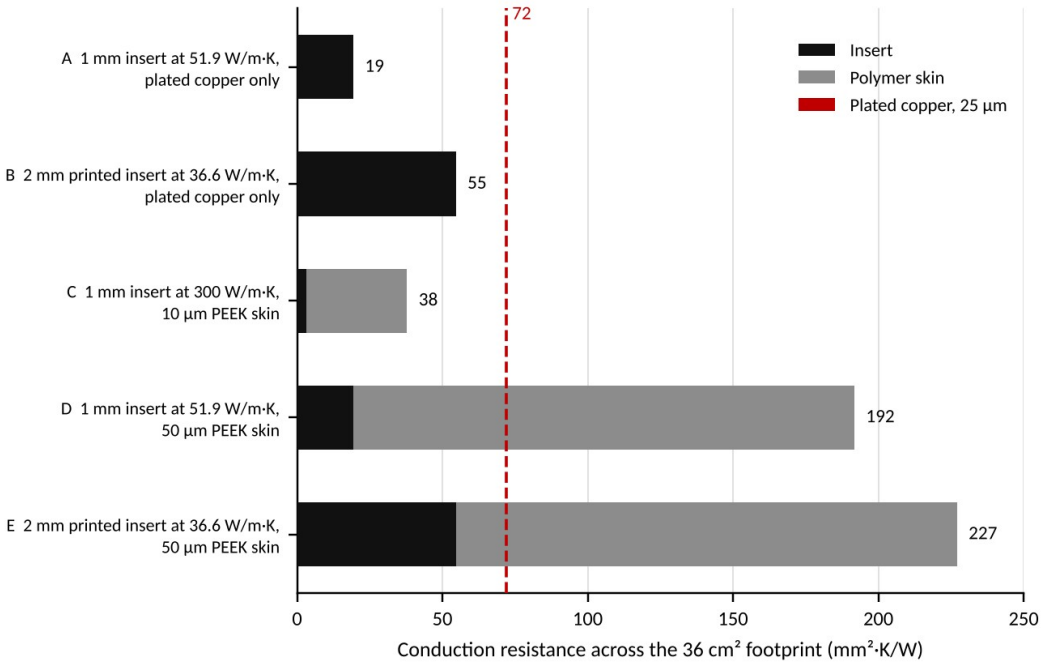

Derived. Builds A to E use the insert conductivities and thicknesses in the text, a copper layer of 25 µm where stated and polymer skins at 0.29 W/m·K. They exclude convection, spreading, contact and bond-line resistance.

7. Erosion of Polymer Surfaces under Jet Impact

7.1 The published water-jet test used a stagnation pressure 632 times the CF-JET case

Mendoza et al. exposed carbon fiber and glass fiber reinforced epoxy plates to a 150 bar water jet at a 75° impact angle and a 65 mm standoff for 10 to 30 minutes.[136] The carbon specimen was an eight-ply 0/90 laminate in Epolam 2015 epoxy, 4 mm thick, and the gelcoated specimens had a polyester gelcoat of 0.56 mm average thickness.[137] The paper reports that the uncoated glass laminate resisted about two times less than the uncoated carbon laminate, and that the gelcoated carbon laminate lost more material than the uncoated carbon laminate.[138] The nozzle diameter and jet velocity are not reported. An ideal Bernoulli estimate for 150 bar gives about 173 m/s and a stagnation pressure of 15 MPa (derived).

Table 8 gives the jet velocity and stagnation pressure for CF-JET flows, with an assumed 100 jets in a 10 by 10 array at 6 mm pitch and a coolant density of 1,030 kg/m^3.[139] A 0.5 mm jet at 8 L/min has a velocity of 6.79 m/s and a stagnation pressure of 23.75 kPa, and a 1 mm jet at 8 L/min has 1.7 m/s and 1.48 kPa (derived). The test of Mendoza et al. had 25.5 times the velocity and 632 times the stagnation pressure of the 0.5 mm case at 8 L/min (derived). The published condition is a conservative screening level, and the erosion rate under it does not transfer to CF-JET, because erosion rate depends on velocity and exposure time in a way that no source quantifies under 10 m/s.

Table 8. Jet velocity and stagnation pressure at the CF-JET flows (derived)

Jet diameter	Total flow (L/min)	Jet velocity (m/s)	Stagnation pressure (kPa)	Ratio of 15 MPa test
0.5 mm	4	3.40	5.94	2,525

Jet diameter	Total flow (L/min)	Jet velocity (m/s)	Stagnation pressure (kPa)	Ratio of 15 MPa test
0.5 mm	8	6.79	23.75	632
1 mm	4	0.85	0.37	40,541
1 mm	8	1.70	1.48	10,135
2 mm	4	0.21	0.02	750,000
2 mm	8	0.42	0.09	166,667

Assumes 100 jets, a coolant density of 1,030 kg/m³ and ideal conversion of the jet velocity head to stagnation pressure. The jet count and array pitch are assumptions of this paper. The last column divides 15 MPa by the stagnation pressure.

Figure 6. Stagnation pressure of CF-JET jets against the published water-jet erosion test

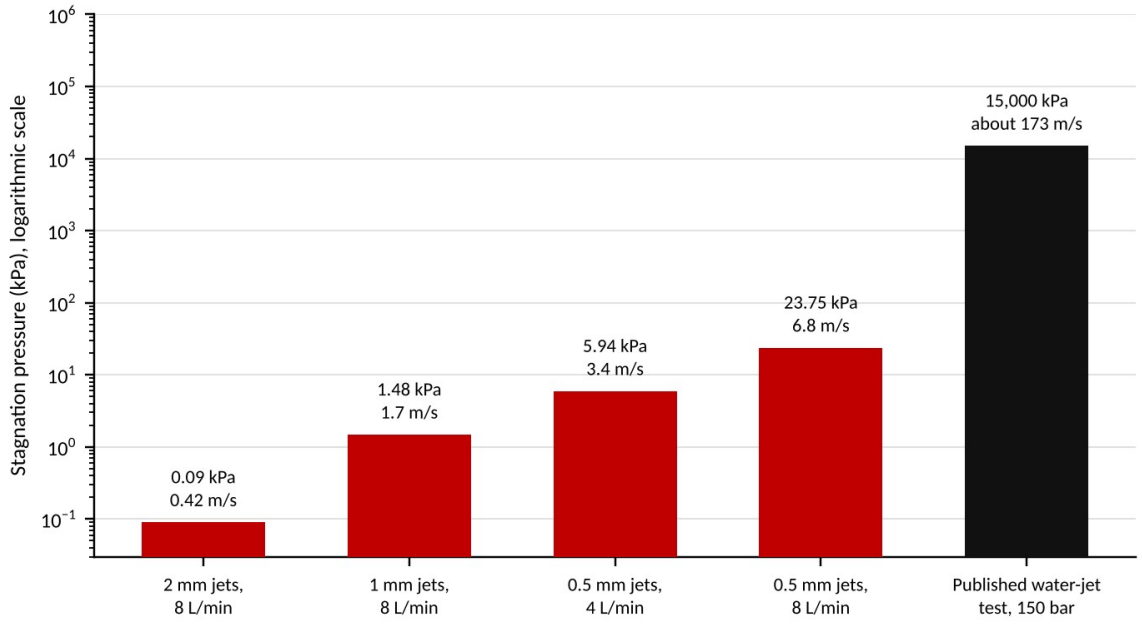

Derived from the jet velocity head. The bars for the CF-JET cases use the assumptions stated for Table 8. The published test value is an ideal Bernoulli estimate for 150 bar.[140]

7.2 Erosion data for slow liquid jets and for thin skins were not found

Cavitation tests give an erosion measure for PEEK, and they apply a different load. Court et al. tested PEEK grades under ASTM G32 vibratory cavitation and report maximum erosion rates of 12.7 to 28.7 µm/h and incubation times of 125 to 156 minutes, and the paper reports two steels as less resistant than PEEK, ceramics and carbide.[141] The data do not translate to an impinging jet at 0.4 to 24 kPa stagnation pressure. No erosion rate for a polymer surface under a liquid jet slower than 10 m/s was found, and no erosion test of a plated or polymer skin of 2 to 50 µm was found, which is an evidence gap. The pressure drop limit of 30 kPa keeps the jet pressures low, and a test at the real velocity with the final face construction over several hundred hours is the measurement that closes the question.

8. Tests of the CF-JET Claims

Table 9 states the verdict for each of the six claims and the basis. Four claims hold within stated conditions,

one is plausible for 50 W/m·K and unsupported for 300 W/m·K, and the skin claim is arithmetically correct and exceeds the budget.

Table 9. Verdicts on the CF-JET target plate claims

Claim	Verdict	Basis
Printed carbon fiber conducts about 1 W/m·K or less through the thickness[142]	Holds for fibers in the plane; unmeasured for printed parts	Laminates at 57% fiber measure 0.76 to 0.89 W/m·K, and pitch fiber laminates at 52% to 75% measure 1.2 to 4.0 W/m·K.[143144] No printed part measurement was found.
Composite density of about 1.5 to 1.8 g/cm³[145]	Holds from about 23% to 55% pitch fiber in PEEK	Rule of mixtures gives 1.36 g/cm³ at 6.42% fiber and 1.78 to 1.80 g/cm³ at 55% (derived). A PAN fiber density was not retrieved.
In-plane expansion of about 0 to 4 ppm/K[146]	Holds along the fibers at 3.6% or more; does not hold across the fibers	Derived with an assumed matrix modulus of 3.6 GPa. The insert region with perpendicular fiber is governed by the 45 to 55 ppm/K matrix in the plane.[147]
Insert through-thickness conductivity of 50 W/m·K or more is attainable, with 300 W/m·K as a ceiling[148]	Plausible and unproven for 50; unsupported for 300	The reported maximum is 51.9 W/m·K in a thin elastomer sheet.[149] Printed pitch fiber reached 36.63 W/m·K at 6.42%.[150] The 300 W/m·K ceiling needs 37.5% to 53.5% fiber (derived).
A plated layer of 10 to 25 µm adds negligible resistance[151]	Holds for copper; bounded for Ni-P	Copper adds 0.03% to 0.09% of the budget, and an illustrative Ni-P case adds 2.8% to 6.9% (derived). Adhesion in hot glycol is unverified.
A 50 µm polymer skin adds about 0.056 K/W[152]	Holds arithmetically at about 0.25 W/m·K; exceeds the budget	The skin is 2.2 to 2.8 times the 0.02 K/W budget (derived). A skin of about 10 µm or less is needed to stay within half of the budget.

Verdicts apply to the evidence retrieved. Derived values use the stated assumptions, and the CF-JET operating point and claims are proposal assumptions.

9. Implications for the CF-JET Effort

9.1 Risks

- **The insert conductivity is unproven at thickness.** The 50 W/m·K claim rests on thin elastomer sheets, and the printed pitch fiber record tops out at 36.63 W/m·K at 6.42 percent fiber.[153154] A 2 mm insert at 36.6 W/m·K uses 76 percent of the budget (derived).
- **Pitch fiber breaks in printing.** The failure strain of 0.4 percent limits the bend radius to about 1.3 mm for a 10.58 µm filament, and commercial printer compatibility with pitch fiber is undocumented.[155]
- **A polymer skin exceeds the budget.** A 50 µm skin adds 2.2 to 2.8 times the 0.02 K/W budget at PEEK conductivities (derived).
- **Plating adhesion in hot glycol is unmeasured.** The adhesion evidence stops at scratch tests, pull-off tests and air cycles to 90 °C, and the 55 to 60 ppm/K normal expansion of the substrate acts on the metal layer.[156157]
- **Matrix durability for PEKK in water-glycol is unmeasured.** PEEK and PEKK have 70 °C or 120 °C water records without glycol, and nylon 66 loses molar mass in glycol at 120 °C or higher.[158159160]
- **Erosion of the face under jets is unmeasured.** The published test had 632 times the stagnation

pressure of the 0.5 mm case at 8 L/min (derived).[161]

9.2 Design implications

- **Specify a high-modulus fiber near 800 W/m·K and measure the tow.** The K13D2U tow measurements of 768 to 792 W/m·K support the value, and K1100 at 576 W/m·K measured shows that listed values can overstate.[162][163]
- **Use a sliced or pin-based insert for the 300 W/m·K case.** Printed inserts at 6.42 percent fiber cannot reach the 37.5 percent that the ceiling needs (derived).
- **Make the plated face the sealed face.** A metal layer of 10 to 25 µm adds under 7 percent of the budget even for Ni-P under the bounding case (derived).
- **Select PEEK for the first builds.** PEEK has the longest hot-water record and a 78 K margin between the coolant inlet and the glass transition onset (derived).[164][165]
- **Keep jets under 1 mm and test the face at the intended velocity.** The 1 and 2 mm jets at 4 to 8 L/min give velocities of 0.21 to 1.7 m/s, and the 0.5 mm jet gives 3.4 to 6.8 m/s (derived, Table 8).
- **Consolidate the printed body and the surface layer.** Compression at 5 bar and 280 °C reduced void content from 12.2 to 1.8 percent in a polyamide system.[166]

9.3 Open research questions

- What through-thickness conductivity does a 1 to 3 mm insert with perpendicular pitch fiber reach at 6, 9, 37 and 55 percent fiber in a PEEK matrix, measured with the plated face and a bond to the plate?
- Can a printer deposit pitch fiber at a bend radius under 1.3 mm without breakage, and what void content results in PEEK?
- What is the adhesion of electroless Ni-P and electroplated copper on carbon fiber PEEK after cycling between dry and 65 °C water-glycol conditions?
- How do PEKK and carbon fiber PEKK behave in 50/50 water-glycol at 65 °C and higher over 1,000 hours?
- What is the erosion rate of a plated and an unplated polymer face under jets of 0.4 to 7 m/s over hundreds of hours?
- How does an insert region with perpendicular fiber alter the local expansion and the stresses at the plated interface?

10. Conclusion

The evidence supports a target plate with a high-modulus pitch fiber body, a plated and sealed face and a perpendicular-fiber insert, and it supports the 72 mm²·K/W budget only if the face skin is about 10 µm or thinner. Axial fiber conductivity is documented at 576 to 800 W/m·K for the pitch grades measured, through-thickness values of 0.76 to 2.8 W/m·K apply to laminates with the fibers in the plane, and aligned fiber interface sheets reach 35.2 to 51.9 W/m·K. The printed pitch fiber record of 36.63 W/m·K at 6.42 percent fiber is the closest measurement to the insert target, and it is a hand-laid sample whose construction needs confirmation.

Of the six claims, the density, expansion and through-thickness conductivity claims hold within stated

limits, the plated layer claim holds for copper, and the 50 µm skin claim is arithmetically correct and exceeds the resistance budget by a factor of 2.2 to 2.8. The 50 W/m·K insert is plausible and the 300 W/m·K ceiling is unsupported. The measurements that decide the design are the thick-insert conductivity, the adhesion of the plated face in hot water-glycol, the pitch fiber printing limit, the PEKK coolant record and the erosion of the face at the real jet velocity.

Bibliography

Ali, Mouaz Mohammed. “High Accuracy Thermal Characterization and Process Improvement for 3D-Printed Continuous Pitch Carbon Fibers.” MASc thesis, York University, 2026. https://yorkspace.library.yorku.ca/items/ce62eede-b9cf-40b9-8d02-dd8444b31e97.

Bard, Simon, Thomas Tran, Florian Schönl, Sabine Rosenfeldt, Martin Demleitner, Holger Ruckdäschel, Markus Retsch, and Volker Altstädt. “Relationship between the Tensile Modulus and the Thermal Conductivity Perpendicular and in Fiber Direction of PAN-Based Carbon Fibers.” *Carbon Letters* 34 (2024): 361–69. https://doi.org/10.1007/s42823-023-00568-2.

Chen, Mudan, Zhaobo Zhang, Bing Zhang, et al. “Electrical and Thermal Behaviour of Z-Pin Reinforced Carbon-Fibre Composite Laminates under Fault Currents.” *Composites Science and Technology* 248 (2024): 110466. https://doi.org/10.1016/j.compscitech.2024.110466.

Court, Spencer, Ilaria Corni, and Nicola Symonds. “Cavitation Erosion Performance of Steel, Ceramics, Carbide, and Victrex PEEK Materials.” *Materials Performance and Characterization* 7, no. 5 (2018). https://store.astm.org/mpc20180027.html.

Dragonplate. Carbon fiber thermal conductivity information page. Vendor material, n.d.

Gao, Shang, Chongyao Wu, Xin Yang, Jirui Cheng, and Renke Kang. “Study on Adhesion Properties and Process Parameters of Electroless Deposited Ni-P Alloy for PEEK and Its Modified Materials.” *Coatings* 13, no. 2 (2023): 388. https://doi.org/10.3390/coatings13020388.

Ibrahim, Yehia, Ahmed Elkholy, J. S. Schofield, G. W. Melenka, and Roger Kempers. “Effective Thermal Conductivity of 3D-Printed Continuous Fiber Polymer Composites.” *Advanced Manufacturing: Polymer & Composites Science* 6 (2020). Cited in the reference list of Olcun, Elkholy, and Kempers (2024); the 4.3 vol% value was not read in the original.

Integran Technologies. U.S. Patents 8,911,878; 8,394,507; 8,916,248; and 8,394,473. Patents on nanocrystalline metallic coatings for polymer and composite substrates. Titles and dates not retrieved.

Klett, James. “High Thermal Conductivity, Mesophase Pitch-Derived Carbon Foams.” Presentation, Oak Ridge National Laboratory, Metals and Ceramics Division, n.d. Archived at https://webarchive.library.unt.edu/eot2008/20090115153011/https:/www.ms.ornl.gov/researchgroups/CMT/foam/Graphite_Foams.pdf.

Laügt, Clément, Jean-Luc Bouvard, Gilles Robert, and Noëlle Billon. “Thermo-Hydro-Glycol Ageing of Polyamide 6,6: Microstructure-Properties Relationships.” *Polymers* 14, no. 19 (2022): 4097. https://doi.org/10.3390/polym14194097.

Li, Baoliu, Yudan Qin, Fang Gao, Chenyu Zhu, Changchun Shan, Jianguang Guo, Zhijun Dong, and Xuanke Li. “Preparation, Microstructure and Thermal Properties of Aligned Mesophase Pitch-Based Carbon Fiber Interface Materials by an Electrostatic Flocking Method.” *Nanomaterials* 14, no. 5 (2024): 393. https://doi.org/10.3390/nano14050393.

Lockheed Martin Corporation. U.S. Patent 6,612,523. Patent describing z-pins for through-thickness thermal conduction, n.d. Title and date not retrieved.

Mendoza Mendoza, Jesus Cornelio, Edgar Ernesto Vera Cardenas, Roger Lewis, William Mai, Erika Osiris Avila Davila,

Armando Irvin Martínez Pérez, Saul Ledesma Ledesma, and Marisa Moreno Rios. “Water Jet Erosion Performance of Carbon Fiber and Glass Fiber Reinforced Polymers.” *Polymers* 13, no. 17 (2021): 2933. https://doi.org/10.3390/polym13172933.

Miller, Sandi G., Paula J. Heimann, Jonathan A. Salem, Ezra O. McNichols, and Kyle Monaghan. *Thermal Conductivity and Mechanical Properties of Epoxy Composites with Hybridized PAN- and Pitch-Based Fiber Architecture*. NASA/TM-20230017100. Cleveland: NASA Glenn Research Center, 2024. https://ntrs.nasa.gov/citations/20230017100.

Mitsubishi Chemical Corporation. Presentation at the 36th seminar of the Carbon Fiber Association (Japan). Vendor material, n.d. carbonfiber.gr.jp.

Nippon Graphite Fiber Co., Ltd. GRANOC pitch-based carbon fiber product information (XN-90 and grade chart). Vendor material, n.d.

Olcun, Sinan, Yehia Ibrahim, Caleb Isaacs, Mohamed Karam, and Ahmed Elkholy. “Thermal Conductivity of 3D-Printed Continuous Pitch Carbon Fiber Composites.” *Additive Manufacturing Letters* (2023): 100106.

Olcun, S., A. Elkholy, and R. Kempers. “High Thermal Conductivity Continuous Pitch Carbon Fiber 3D Printed Using a 6-Axis Robot Arm.” *Progress in Additive Manufacturing* (2024). https://doi.org/10.1007/s40964-024-00568-2.

Olcun, Sinan. “Development of Characterization of 3D-Printed Continuous Pitch Carbon Fiber Composites.” MASc thesis, York University, 2023. https://hdl.handle.net/10315/41593.

Report Y-2269. Oak Ridge, TN: U.S. Department of Energy, Office of Scientific and Technical Information, 1982. Title not retrieved.

Parker, M., N. Ezeokeke, R. Matsuzaki, and D. Arola. “Strength and Its Variability in 3D Printing of Polymer Composites with Continuous Fibers.” *Materials & Design* 225 (2023): 111505.

Porto, Geilza Alves, Luiz Guilherme Abreu de Paula, Jose Jonathan Rubio Arias, Erica Gervasoni Chaves, et al. “Comparative Analysis of Poly(Ether-Ether-Ketone) Properties Aged in Different Conditions for Application in Pipelines.” *Journal of Thermal Analysis and Calorimetry* 148 (2023): 79–95. https://doi.org/10.1007/s10973-022-11582-3.

Purdue University, CMS Phase II Tracker Upgrade group. “Thermal Measurements.” Web page, n.d. https://physics.purdue.edu/cmsfpix/ThermalMeasurements.

Scruggs, Kirmse, and Hsiao. “Enhancement of Through-Thickness Thermal Transport in Unidirectional Carbon Fiber Reinforced Plastic Laminates due to the Synergetic Role of Carbon Nanofiber Z-Threads.” *Journal of Nanomaterials* 2019: 1–13. https://par.nsf.gov/biblio/10096110. Author names as recorded in the project research notes; the repository page lists no authors.

Senis, Evangelos C., Igor O. Golosnoy, Janice M. Dulieu-Barton, and Ole T. Thomsen. “Characterization of Through-Thickness Thermal Conductivity of Wind Turbine Blade CFRP Materials Using a Steady-State Technique.” Paper presented at the 21st International Conference on Composite Materials, Xi’an, 20–25 August 2017. https://eprints.soton.ac.uk/417840/.

SOL Engineering Services, LLC. *CF-JET: AI/ML-Enabled Design and Development of an Additively Manufactured, Liquid-Cooled Jet-Impingement Cold Plate with Optimized Carbon Fiber Target Plate*. Proposal, Rev Final 2, n.d.

Şükür, Emine Feyza, Sinem Elmas, Mahsa Seyednourani, Volkan Eskizeybek, Mehmet Yıldız, and Hatice Sinem Şaş Çaycı. “A Rational Study on the Hydrothermal Aging of AFP Manufactured CF/Polyetherketoneketone Composites with In Situ Consolidation Supported by Acoustic Emission Inspection.” *Journal of Applied Polymer Science* 139, no. 29 (2022): e52480. https://doi.org/10.1002/app.52480.

Thomason, J. L., J. Z. Ali, and J. Anderson. “Effects of Hydrolysis Ageing on the Performance and Dimensional Stability of Glass-Fiber Reinforced Polyamide 66.” Paper presented at ANTEC 2010, Orlando, 16–20 June 2010. https://strathprints.strath.ac.uk/id/eprint/20623.

Thomason, J. L., and G. Porteus. “Swelling of Glass-Fibre Reinforced Polyamide 66 during Conditioning in Water, Ethylene

Glycol and Antifreeze Mixture." *Polymer Composites* 32, no. 4 (2011): 639–47. https://doi.org/10.1002/pc.21054.

Victrex plc. VICTREX PEEK 450G datasheet. Vendor material, n.d.

Wilt, Jackson K., Nadim S. Hmeidat, John W. Bohling, and Brett G. Compton. "High Through-Thickness Thermal Conductivity of 3D-Printed Composites via Rotational Direct Ink Writing." *Additive Manufacturing Letters* 7 (2023): 100167. https://doi.org/10.1016/j.addlet.2023.100167.

Xu, Xiangyu, Baoyan Zhang, Fenghui Shi, Kai Liu, Gongqiu Peng, and Junpeng Gao. "Study on the Mechanical Properties of Carbon Fabric/Polyetherketoneketone Composites under Different Environmental Conditions." *Polymers* 17, no. 9 (2025): 1142. https://doi.org/10.3390/polym17091142.

Youngblood, G. E., D. J. Senor, W. Kowbel, J. Webb, and A. Kohyama. "Thermal Conductivity of SiC and C Fibers." In *Fusion Materials: Semi-Annual Progress Report Ending December 31, 1999*, edited by A. F. Rowcliffe, 113–18. Washington, DC: U.S. Department of Energy, Office of Fusion Energy Sciences, 2000. PNNL-SA-31870. https://www.osti.gov/biblio/984292.

Yu, Zifeng, et al. Thermal interface material with electrostatically flocked mesophase pitch carbon fibers. *Journal of Materials Science: Materials in Electronics* (2019). https://doi.org/10.1007/s10854-019-01360-7. The article title was not retrieved; the first author is as given in the citing paper.

Yudhanto, Arief, Alwaleed Aldhirgham, Eric Feron, and Gilles Lubineau. "Post-Consolidation Process for Modifying Microscale and Mesoscale Parameters of 3D Printed Composite Materials." *Frontiers in Materials* 10 (2023). https://doi.org/10.3389/fmats.2023.1286840.

Zhang, Zhenbang, Maohua Li, Yandong Wang, Wen Dai, Linhong Li, Yapeng Chen, Xiangdong Kong, et al. "Ultrahigh Thermal Conductive Polymer Composites by the 3D Printing Induced Vertical Alignment of Carbon Fiber." *Journal of Materials Chemistry A* 11, no. 20 (2023): 10971–83. https://doi.org/10.1039/D3TA01676E.

Zhang, Zhenbang, Rongjie Yang, Yandong Wang, Kang Xu, Wen Dai, Jianxiang Zhang, Maohua Li, et al. "Enhanced Thermal Conductivity and Reduced Thermal Resistance in Carbon Fiber-Based Thermal Interface Materials with Vertically Aligned Structure." *Journal of Materials Chemistry A* 12 (2024): 24428–40. https://doi.org/10.1039/D4TA03924F.

Notes

[1]Zhenbang Zhang et al., “Ultrahigh Thermal Conductive Polymer Composites by the 3D Printing Induced Vertical Alignment of Carbon Fiber,” *Journal of Materials Chemistry A* 11, no. 20 (2023): 10971–83, https://doi.org/10.1039/D3TA01676E.

[2]Zhenbang Zhang et al., “Enhanced Thermal Conductivity and Reduced Thermal Resistance in Carbon Fiber-Based Thermal Interface Materials with Vertically Aligned Structure,” *Journal of Materials Chemistry A* 12 (2024): 24428–40, https://doi.org/10.1039/D4TA03924F.

[3]Evangelos C. Senis et al., “Characterization of Through-Thickness Thermal Conductivity of Wind Turbine Blade CFRP Materials Using a Steady-State Technique,” paper presented at the 21st International Conference on Composite Materials, Xi’an, 20–25 August 2017, https://eprints.soton.ac.uk/417840/.

[4]Purdue University, CMS Phase II Tracker Upgrade group, “Thermal Measurements,” web page, n.d., https://physics.purdue.edu/cmsfpix/ThermalMeasurements.

[5]SOL Engineering Services, LLC, *CF-JET: AI/ML-Enabled Design and Development of an Additively Manufactured, Liquid-Cooled Jet-Impingement Cold Plate with Optimized Carbon Fiber Target Plate*, proposal, Rev Final 2, n.d.

[6]G. E. Youngblood et al., “Thermal Conductivity of SiC and C Fibers,” in *Fusion Materials: Semi-Annual Progress Report Ending December 31, 1999*, ed. A. F. Rowcliffe (Washington, DC: U.S. Department of Energy, Office of Fusion Energy Sciences, 2000), 113–18, PNNL-SA-31870, https://www.osti.gov/biblio/984292.

[7]Mouaz Mohammed Ali, “High Accuracy Thermal Characterization and Process Improvement for 3D-Printed Continuous Pitch Carbon Fibers” (MASc thesis, York University, 2026), https://yorkspace.library.yorku.ca/items/ce62eede-b9cf-40b9-8d02-dd8444b31e97.

[8]Simon Bard et al., “Relationship between the Tensile Modulus and the Thermal Conductivity Perpendicular and in Fiber Direction of PAN-Based Carbon Fibers,” *Carbon Letters* 34 (2024): 361–69, https://doi.org/10.1007/s42823-023-00568-2.

[9]Ali, “3D-Printed Continuous Pitch Carbon Fibers.”

[10]Arief Yudhanto et al., “Post-Consolidation Process for Modifying Microscale and Mesoscale Parameters of 3D Printed Composite Materials,” *Frontiers in Materials* 10 (2023), https://doi.org/10.3389/fmats.2023.1286840.

[11]Geilza Alves Porto et al., “Comparative Analysis of Poly(Ether-Ether-Ketone) Properties Aged in Different Conditions for Application in Pipelines,” *Journal of Thermal Analysis and Calorimetry* 148 (2023): 79–95, https://doi.org/10.1007/s10973-022-11582-3.

[12]Clément Laügt et al., “Thermo-Hydro-Glycol Ageing of Polyamide 6,6: Microstructure-Properties Relationships,” *Polymers* 14, no. 19 (2022): 4097, https://doi.org/10.3390/polym14194097.

[13]Jesus Cornelio Mendoza Mendoza et al., “Water Jet Erosion Performance of Carbon Fiber and Glass Fiber Reinforced Polymers,” *Polymers* 13, no. 17 (2021): 2933, https://doi.org/10.3390/polym13172933.

[14]SOL Engineering Services, *CF-JET*, Rev Final 2.

[15]SOL Engineering Services, *CF-JET*, Rev Final 2.

[16]SOL Engineering Services, *CF-JET*, Rev Final 2.

[17]Mitsubishi Chemical Corporation, presentation at the 36th seminar of the Carbon Fiber Association (Japan), vendor material, n.d., carbonfiber.gr.jp.

[18]Ali, “3D-Printed Continuous Pitch Carbon Fibers.”

[19]Ali, “3D-Printed Continuous Pitch Carbon Fibers.”

[20]Youngblood et al., “Thermal Conductivity of SiC and C Fibers.”

[21]James Klett, “High Thermal Conductivity, Mesophase Pitch-Derived Carbon Foams,” presentation, Oak Ridge National Laboratory, Metals and Ceramics Division, n.d., archived at https://webarchive.library.unt.edu/eot2008/20090115153011/https:/www.ms.ornl.gov/researchgroups/CMT/foam/Graphite_Foams.pdf.

[22]Nippon Graphite Fiber Co., Ltd., GRANOC pitch-based carbon fiber product information (XN-90 and grade chart), vendor material, n.d.

[23]Sandi G. Miller et al., *Thermal Conductivity and Mechanical Properties of Epoxy Composites with Hybridized PAN- and Pitch-Based Fiber Architecture*, NASA/TM-20230017100 (Cleveland: NASA Glenn Research Center, 2024), https://ntrs.nasa.gov/citations/20230017100.

[24]Youngblood et al., “Thermal Conductivity of SiC and C Fibers.”

[25]Klett, “Mesophase Pitch-Derived Carbon Foams.”

[26]Mitsubishi Chemical, Carbon Fiber Association seminar presentation.

[27]Ali, “3D-Printed Continuous Pitch Carbon Fibers.”

[28]Nippon Graphite Fiber, GRANOC product information.

[29]Nippon Graphite Fiber, GRANOC product information.

[30]Miller et al., *Hybridized PAN- and Pitch-Based Fiber Architecture*.

[31]Klett, “Mesophase Pitch-Derived Carbon Foams.”

[32]Bard et al., “Tensile Modulus and Thermal Conductivity of PAN-Based Carbon Fibers.”

[33]Bard et al., “Tensile Modulus and Thermal Conductivity of PAN-Based Carbon Fibers.”

[34]Nippon Graphite Fiber, GRANOC product information.

[35]Dragonplate, carbon fiber thermal conductivity information page, vendor material, n.d.

[36]Bard et al., “Tensile Modulus and Thermal Conductivity of PAN-Based Carbon Fibers.”

[37]Bard et al., “Tensile Modulus and Thermal Conductivity of PAN-Based Carbon Fibers.”

[38]Bard et al., “Tensile Modulus and Thermal Conductivity of PAN-Based Carbon Fibers.”

[39]Purdue University, “Thermal Measurements.”

[40]Senis et al., “Through-Thickness Thermal Conductivity of Wind Turbine Blade CFRP.”

[41]Purdue University, “Thermal Measurements.”

[42]Miller et al., *Hybridized PAN- and Pitch-Based Fiber Architecture*.

[43]Senis et al., “Through-Thickness Thermal Conductivity of Wind Turbine Blade CFRP.”

[44]Purdue University, “Thermal Measurements.”

[45]Purdue University, “Thermal Measurements.”

[46]Purdue University, “Thermal Measurements.”

[47]Scruggs, Kirmse, and Hsiao, “Enhancement of Through-Thickness Thermal Transport in Unidirectional Carbon Fiber Reinforced Plastic Laminates due to the Synergetic Role of Carbon Nanofiber Z-Threads,” *Journal of Nanomaterials* 2019: 1–13, https://par.nsf.gov/biblio/10096110.

[48]Scruggs, Kirmse, and Hsiao, “Carbon Nanofiber Z-Threads.”

[49]Scruggs, Kirmse, and Hsiao, “Carbon Nanofiber Z-Threads.”

[50]Miller et al., *Hybridized PAN- and Pitch-Based Fiber Architecture*.

[51]Jackson K. Wilt et al., “High Through-Thickness Thermal Conductivity of 3D-Printed Composites via Rotational Direct Ink Writing,” *Additive Manufacturing Letters* 7 (2023): 100167, https://doi.org/10.1016/j.addlet.2023.100167.

[52]Victrex plc, VICTREX PEEK 450G datasheet, vendor material, n.d.

[53]Ali, “3D-Printed Continuous Pitch Carbon Fibers.”

[54]Sinan Olcun et al., “Thermal Conductivity of 3D-Printed Continuous Pitch Carbon Fiber Composites,” *Additive Manufacturing Letters* (2023): 100106.

[55]Yehia Ibrahim et al., “Effective Thermal Conductivity of 3D-Printed Continuous Fiber Polymer Composites,” *Advanced Manufacturing: Polymer & Composites Science* 6 (2020), as cited in the reference list of Olcun, Elkholy, and Kempers (2024).

[56]Ali, “3D-Printed Continuous Pitch Carbon Fibers.”

[57]Olcun et al., “Thermal Conductivity of 3D-Printed Continuous Pitch Carbon Fiber Composites.”

[58]Ibrahim et al., “Effective Thermal Conductivity of 3D-Printed Continuous Fiber Polymer Composites.”

[59]Victrex, PEEK 450G datasheet.

[60]Ali, “3D-Printed Continuous Pitch Carbon Fibers.”

[61]Mitsubishi Chemical, Carbon Fiber Association seminar presentation.

[62]Victrex, PEEK 450G datasheet.

[63]Victrex, PEEK 450G datasheet.

[64]Zifeng Yu et al., thermal interface material with electrostatically flocked mesophase pitch carbon fibers, *Journal of Materials Science: Materials in Electronics* (2019), https://doi.org/10.1007/s10854-019-01360-7.

[65]Baoliu Li et al., “Preparation, Microstructure and Thermal Properties of Aligned Mesophase Pitch-Based Carbon Fiber Interface Materials by an Electrostatic Flocking Method,” *Nanomaterials* 14, no. 5 (2024): 393, https://doi.org/10.3390/nano14050393.

[66]Zhang et al., “3D Printing Induced Vertical Alignment of Carbon Fiber.”

[67]Zhang et al., “Carbon Fiber-Based Thermal Interface Materials with Vertically Aligned Structure.”

[68]Zhang et al., “3D Printing Induced Vertical Alignment of Carbon Fiber.”

[69]Zhang et al., “Carbon Fiber-Based Thermal Interface Materials with Vertically Aligned Structure.”

[70]Yu et al., flocked mesophase pitch carbon fiber interface material.

[71]Li et al., “Aligned Mesophase Pitch-Based Carbon Fiber Interface Materials.”

[72]Mudan Chen et al., “Electrical and Thermal Behaviour of Z-Pin Reinforced Carbon-Fibre Composite Laminates under Fault Currents,” *Composites Science and Technology* 248 (2024): 110466, https://doi.org/10.1016/j.compscitech.2024.110466.

[73]Lockheed Martin Corporation, U.S. Patent 6,612,523, patent describing z-pins for through-thickness thermal conduction, n.d. (title and date not retrieved).

[74]Scruggs, Kirmse, and Hsiao, “Carbon Nanofiber Z-Threads.”

[75]Wilt et al., “Rotational Direct Ink Writing.”

[76]Miller et al., *Hybridized PAN- and Pitch-Based Fiber Architecture*.

[77]Chen et al., “Z-Pin Reinforced Carbon-Fibre Composite Laminates under Fault Currents.”

[78]Lockheed Martin, U.S. Patent 6,612,523.

[79]Chen et al., “Z-Pin Reinforced Carbon-Fibre Composite Laminates under Fault Currents.”

[80]Zhang et al., “Carbon Fiber-Based Thermal Interface Materials with Vertically Aligned Structure.”

[81]Purdue University, “Thermal Measurements.”

[82]Mitsubishi Chemical, Carbon Fiber Association seminar presentation.

[83]Ali, “3D-Printed Continuous Pitch Carbon Fibers.”

[84]Ali, “3D-Printed Continuous Pitch Carbon Fibers.”

[85]S. Olcun, A. Elkholy, and R. Kempers, “High Thermal Conductivity Continuous Pitch Carbon Fiber 3D Printed Using a 6-Axis Robot Arm,” *Progress in Additive Manufacturing* (2024), https://doi.org/10.1007/s40964-024-00568-2.

[86]Ali, “3D-Printed Continuous Pitch Carbon Fibers.”

[87]Ali, “3D-Printed Continuous Pitch Carbon Fibers.”

[88]Ali, “3D-Printed Continuous Pitch Carbon Fibers.”

[89]Sinan Olcun, “Development of Characterization of 3D-Printed Continuous Pitch Carbon Fiber Composites” (MASc thesis, York University, 2023), https://hdl.handle.net/10315/41593.

[90]Olcun, Elkholy, and Kempers, “6-Axis Robot Arm.”

[91]M. Parker et al., “Strength and Its Variability in 3D Printing of Polymer Composites with Continuous Fibers,” *Materials & Design* 225 (2023): 111505.

[92]Parker et al., “Strength and Its Variability in 3D Printing.”

[93]Yudhanto et al., “Post-Consolidation Process.”

[94]Yudhanto et al., “Post-Consolidation Process.”

[95]Olcun et al., “Thermal Conductivity of 3D-Printed Continuous Pitch Carbon Fiber Composites.”

[96]Olcun, “Continuous Pitch Carbon Fiber Composites.”

[97]Ibrahim et al., “Effective Thermal Conductivity of 3D-Printed Continuous Fiber Polymer Composites.”

[98]Ali, “3D-Printed Continuous Pitch Carbon Fibers.”

[99]Olcun, Elkholy, and Kempers, “6-Axis Robot Arm.”

[100]Parker et al., “Strength and Its Variability in 3D Printing.”

[101]Yudhanto et al., “Post-Consolidation Process.”

[102]Victrex, PEEK 450G datasheet.

[103]Porto et al., “PEEK Properties Aged in Different Conditions.”

[104]Porto et al., “PEEK Properties Aged in Different Conditions.”

[105]Xiangyu Xu et al., “Study on the Mechanical Properties of Carbon Fabric/Polyetherketoneketone Composites under Different Environmental Conditions,” *Polymers* 17, no. 9 (2025): 1142, https://doi.org/10.3390/polym17091142.

[106]Xu et al., “Carbon Fabric/PEKK Composites under Different Environmental Conditions.”

[107]Emine Feyza Şükür et al., “A Rational Study on the Hydrothermal Aging of AFP Manufactured CF/Polyetherketoneketone Composites with In Situ Consolidation Supported by Acoustic Emission Inspection,” *Journal of Applied Polymer Science* 139, no. 29 (2022): e52480, https://doi.org/10.1002/app.52480.

[108]Laügt et al., “Thermo-Hydro-Glycol Ageing of Polyamide 6,6.”

[109]Laügt et al., “Thermo-Hydro-Glycol Ageing of Polyamide 6,6.”

[110]Laügt et al., “Thermo-Hydro-Glycol Ageing of Polyamide 6,6.”

[111]J. L. Thomason, J. Z. Ali, and J. Anderson, “Effects of Hydrolysis Ageing on the Performance and Dimensional Stability of Glass-Fiber Reinforced Polyamide 66,” paper presented at ANTEC 2010, Orlando, 16–20 June 2010, https://strathprints.strath.ac.uk/id/eprint/20623.

[112]J. L. Thomason and G. Porteus, “Swelling of Glass-Fibre Reinforced Polyamide 66 during Conditioning in Water, Ethylene Glycol and Antifreeze Mixture,” *Polymer Composites* 32, no. 4 (2011): 639–47, https://doi.org/10.1002/pc.21054.

[113]Victrex, PEEK 450G datasheet.

[114]Porto et al., “PEEK Properties Aged in Different Conditions.”

[115]Xu et al., “Carbon Fabric/PEKK Composites under Different Environmental Conditions.”

[116]Şükür et al., “Hydrothermal Aging of AFP Manufactured CF/PEKK Composites.”

[117]Laügt et al., “Thermo-Hydro-Glycol Ageing of Polyamide 6,6.”

[118]Thomason, Ali, and Anderson, “Hydrolysis Ageing of Glass-Fiber Reinforced Polyamide 66.”

[119]Thomason and Porteus, “Swelling of Glass-Fibre Reinforced Polyamide 66.”

[120]SOL Engineering Services, *CF-JET*, Rev Final 2.

[121]Shang Gao et al., “Study on Adhesion Properties and Process Parameters of Electroless Deposited Ni-P Alloy for PEEK and Its Modified Materials,” *Coatings* 13, no. 2 (2023): 388, https://doi.org/10.3390/coatings13020388.

[122]Gao et al., “Electroless Deposited Ni-P Alloy for PEEK.”

[123]Gao et al., “Electroless Deposited Ni-P Alloy for PEEK.”

[124]Integran Technologies, U.S. Patents 8,911,878; 8,394,507; 8,916,248; and 8,394,473, patents on nanocrystalline metallic coatings for polymer and composite substrates (titles and dates not retrieved).

[125]Integran Technologies, U.S. Patents 8,911,878; 8,394,507; 8,916,248; 8,394,473.

[126]Mitsubishi Chemical, Carbon Fiber Association seminar presentation.

[127]Report Y-2269 (Oak Ridge, TN: U.S. Department of Energy, Office of Scientific and Technical Information, 1982) (title not retrieved).

[128]Victrex, PEEK 450G datasheet.

[129]Yu et al., flocked mesophase pitch carbon fiber interface material.

[130]Li et al., “Aligned Mesophase Pitch-Based Carbon Fiber Interface Materials.”

[131]Zhang et al., “3D Printing Induced Vertical Alignment of Carbon Fiber.”

[132]Ali, “3D-Printed Continuous Pitch Carbon Fibers.”

[133]Zhang et al., “Carbon Fiber-Based Thermal Interface Materials with Vertically Aligned Structure.”

[134]SOL Engineering Services, *CF-JET*, Rev Final 2.

[135]SOL Engineering Services, *CF-JET*, Rev Final 2.

[136]Mendoza et al., “Water Jet Erosion Performance.”

[137]Mendoza et al., “Water Jet Erosion Performance.”

[138]Mendoza et al., “Water Jet Erosion Performance.”

[139]SOL Engineering Services, *CF-JET*, Rev Final 2.

[140]Mendoza et al., “Water Jet Erosion Performance.”

[141]Spencer Court, Ilaria Corni, and Nicola Symonds, “Cavitation Erosion Performance of Steel, Ceramics, Carbide, and Victrex PEEK Materials,” *Materials Performance and Characterization* 7, no. 5 (2018), https://store.astm.org/mpc20180027.html.

[142]SOL Engineering Services, *CF-JET*, Rev Final 2.

[143]Senis et al., “Through-Thickness Thermal Conductivity of Wind Turbine Blade CFRP.”

[144]Purdue University, “Thermal Measurements.”

[145]SOL Engineering Services, *CF-JET*, Rev Final 2.

[146]SOL Engineering Services, *CF-JET*, Rev Final 2.

[147]Victrex, PEEK 450G datasheet.

[148]SOL Engineering Services, *CF-JET*, Rev Final 2.

[149]Zhang et al., “Carbon Fiber-Based Thermal Interface Materials with Vertically Aligned Structure.”

[150]Ali, “3D-Printed Continuous Pitch Carbon Fibers.”

[151]SOL Engineering Services, *CF-JET*, Rev Final 2.

[152]SOL Engineering Services, *CF-JET*, Rev Final 2.

[153]Zhang et al., “Carbon Fiber-Based Thermal Interface Materials with Vertically Aligned Structure.”

[154]Ali, “3D-Printed Continuous Pitch Carbon Fibers.”

[155]Ali, “3D-Printed Continuous Pitch Carbon Fibers.”

[156]Gao et al., “Electroless Deposited Ni-P Alloy for PEEK.”

[157]Integran Technologies, U.S. Patents 8,911,878; 8,394,507; 8,916,248; 8,394,473.

[158]Porto et al., “PEEK Properties Aged in Different Conditions.”

[159]Xu et al., “Carbon Fabric/PEKK Composites under Different Environmental Conditions.”

[160]Laügt et al., “Thermo-Hydro-Glycol Ageing of Polyamide 6,6.”

[161]Mendoza et al., “Water Jet Erosion Performance.”

[162]Ali, “3D-Printed Continuous Pitch Carbon Fibers.”

[163]Youngblood et al., “Thermal Conductivity of SiC and C Fibers.”

[164]Porto et al., “PEEK Properties Aged in Different Conditions.”

[165]Victrex, PEEK 450G datasheet.

[166]Yudhanto et al., “Post-Consolidation Process.”